

EPR Studies of the Near-Surface Layer in a Dilute Gold-Erbium Alloy

A. Raizman and J. T. Suss

Solid State Physics Department, Soreq Nuclear Research Centre, Yavne 70600, Israel

and

D. N. Seidman

Department of Materials Science and Engineering, Cornell University, Ithaca, New York 14853

and

D. Shaltiel

The Racah Institute of Physics, The Hebrew University, Jerusalem, Israel

and

V. Zevin

The Racah Institute of Physics, The Hebrew University, Jerusalem, Israel, and Max-Planck-Institut für Festkörperforschung, D-7000 Stuttgart 80, Germany

(Received 19 August 1980)

Annealing a foil of a dilute Au:Er alloy at 400 C produced a near-surface layer approximately 0.5 μm thick, with properties different from those of the bulk. These results were obtained using the electron-paramagnetic-resonance (EPR) technique. A theory for the EPR line shape was developed which showed that the A/B ratio of a paramagnetic impurity in a metal can vary when a near-surface layer exists. The theoretical results may explain anomalous A/B ratios observed in EPR experiments on other dilute metal alloys.

PACS numbers: 76.30.Kg, 81.40.Ef, 81.40.Rs

In the course of a study of defects produced by cold working (rolling and mechanical polishing) in dilute gold-erbium alloys, with use of the electron-paramagnetic-resonance (EPR) technique,¹ we observed significant changes in the asymmetry parameter A/B [the ratio between the maximum and minimum of the first derivative of the resonance line; for a definition, see Fig. 1(a) of Ref. 1], the linewidth (ΔH), and the intensity (I) of the resonance line in samples which were annealed, as compared with unannealed samples. The A/B ratio increased after annealing, but ΔH and I decreased. Typical spectra of Er in Au in a rolled and annealed sample demonstrating these changes are shown in Fig. 1 of Ref. 1. Large A/B ratios for impurities in a metal host have been reported previously.^{2,3} The existing theories concerning paramagnetic impurities in a dilute alloy do not explain the large A/B ratios observed. In this work, we have analyzed the unusual features of the EPR line of Er in Au in terms of a model consisting of a near-surface layer and the bulk.

The sample preparation and the EPR spectrometer were described in Ref. 1. For the determination of I , we used the parameter $I = (A + B)$

$(\Delta H)^2$, which is proportional to the integrated intensity of the resonance line; the value of ΔH was the linewidth at $A/2$. ΔH of Er in Au, as a function of temperature T , can be expressed, in our range of T , as $\Delta H = a + bT$, where a represents the residual linewidth and b the thermal broadening of the linewidth (the Korringa relaxation rate). In order to obtain an understanding of the changes in the EPR line shape, we performed two types of experiments:

Successive etching.—In a Au sample with a nominal concentration of 2000 ppm Er, annealed for one hour at 400 C, thin layers approximately 0.1 μm thick were removed successively by etching with dilute aqua regia, and the thickness of the layer removed was determined by accurately weighing the sample. The EPR line of Er was recorded after each etching treatment to obtain the depth profile of ΔH and of the A/B ratio. The results are plotted in Fig. 1. In the rolled sample, $\Delta H = 52$ G and $A/B = 3$, at 1.65 K. Etching away 0.5 μm of the surface of the sample recovered about 80% of ΔH of the rolled sample before annealing. No appreciable further recovery was obtained by increasing the thickness of the etched layer to 2 μm . The A/B ratio recovered

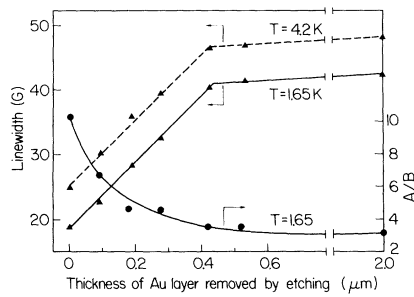


FIG. 1. The EPR linewidth ΔH and the A/B ratio in a heated sample of Au doped with 2000 ppm Er, as a function of the thickness of a surface layer removed by successive etching. The lines only serve as a guide to the eye.

completely after etching away $0.5 \mu\text{m}$ of metal. After etching, most of I was recovered (as compared with the value before annealing). These results demonstrated that annealing the sample for one hour at 400 C affected mainly a near-surface layer with a thickness of approximately $0.5 \mu\text{m}$.

Isothermal annealing.—The behavior of ΔH , A/B , and I in a rolled sample of Au with a nominal concentration of 2000 ppm Er was studied as a function of isothermal annealing time. The sample was annealed at 400 C in an open quartz ampule, each time for several minutes, and ΔH , A/B , and I were recorded as a function of the heating time. After each annealing step, the sample was quenched to room temperature by immersing the ampule in water. Heating the sample in air had about the same effect on the resonance line as heating in vacuum. The results are plotted in Fig. 2.

The main puzzle of the experimental results is the anomalous A/B ratio of the EPR signal. The independence of b on the Er concentration and on the thermal and mechanical treatments, and a large difference between the g factor of the Er ions and that of the conduction electrons indicate that the EPR signal in Au:Er is not bottlenecked and is not a sort of combined (hybridized) impurity-conduction-electron resonance. Therefore the conduction electrons in Au:Er serve mainly as a thermal bath. The role of the diffusion of the Er magnetization is also negligible for the impurity concentration employed.

The etching experiment suggests the following model to explain the changes produced by heating in the features of the EPR line of Er in Au. We assume the existence of a near-surface layer

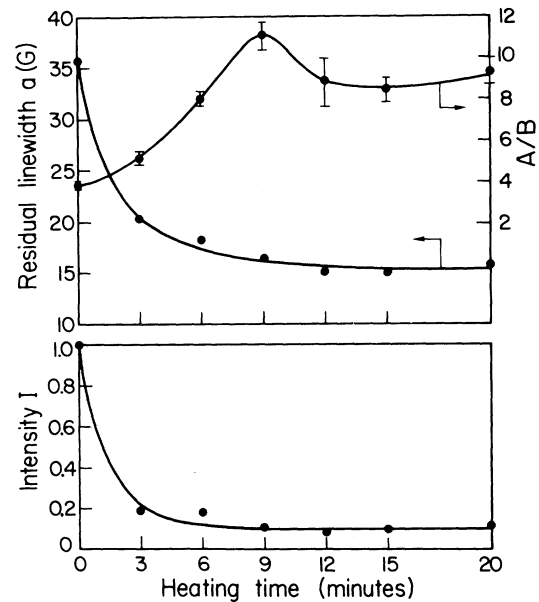


FIG. 2. Isothermal annealing at 400 C of a rolled sample of Au + 2000 ppm Er. The error bars represent the variation of A/B between 1.6 and 4.2 K. I was calculated with use of data recorded at 1.65 K. The lines serve only as a guide to the eye.

with properties different from those of the bulk. We use a simplification of a homogeneous layer on a homogeneous bulk, each having a different conductivity σ_1 and σ_2 and a different skin depth δ_1 and δ_2 , respectively. σ_2 is identical to that of the rolled sample before heating, and is determined mainly by the concentration c_2 of the Er ions (the contribution to the resistivity is $\approx 7 \mu\Omega \text{ cm/at.}\%$ Er) and it is assumed that almost all of the Er ions before heating are at cubic sites and contribute to the EPR linewidth and intensity. σ_1 is determined by the concentration c_1 of the Er ions at cubic sites and also by the Er ions trapped by dislocations. The strong decrease in the intensity of the resonance line after heating clearly shows that the number of Er ions contributing to the resonance line has been reduced by heating ($c_1 < c_2$). In the following, we keep σ_1 independent of c_1 .

To obtain the surface impedance⁴ of the Au:Er sample we assume plane geometry with the z axis perpendicular to the sample surface and the field vectors of the form $Ae^{-i(\omega t + kz)}$. Here $A (=A_x - iA_y)$ stands for E , H , and M , the electric and magnetic rf fields and the impurity magnetization, respectively. Simultaneously solving the Maxwell equations with the simplified Bloch-

Hasegawa equations^{5,6}

$$[iT_{2j}(\omega - \omega_0) + 1]M_j + T_{2j}\omega_0\chi_j^0 H_j = 0, \quad j=1, 2, \quad (1)$$

and using the obvious boundary conditions at $z=d$ and $z \rightarrow \infty$, one can calculate the energy absorbed, which is proportional to the real part of the surface impedance, i.e., $\text{Im}[E(z=0)/H(z=0)]$ in our case. In Eq. (1), $j=1, 2$ corresponds to the layer and bulk, respectively, d is the layer thickness, χ^0 is the static susceptibility of the Er ions which contribute to the EPR, $\omega_0 = g\mu_B H/\hbar$ is the Er^{3+} resonance frequency in the static magnetic field H , g is the Er^{3+} g factor, μ_B is the Bohr magneton, and T_2^{-1} is the phenomenological linewidth. The result is

$$\text{Im}\left(\frac{E(z=0)}{H(z=0)}\right) = \text{Re}\left(\frac{ck_2}{4\pi\sigma_2} \frac{(k_1\sigma_2/k_2\sigma_1)\tanh(k_1d) + 1}{(k_2\sigma_1/k_1\sigma_2)\tanh(k_1d) + 1}\right), \quad (2)$$

with

$$k_j = \frac{\sqrt{2}}{\delta_j} \left[i + \frac{4\pi T_{2j}\omega_0\chi_j^0}{iT_2(\omega - \omega_0) + 1} \right]^{1/2} \approx \frac{1+i}{\delta_j} \left(1 - i \frac{2\pi T_{2j}\omega_0\chi_j^0}{iT_2(\omega - \omega_0) + 1} \right). \quad (3)$$

To obtain the power P_m which the sample absorbs per unit area because of the magnetic impurities, we expand Eq. (2) by using Eq. (3) to give

$$P_m \propto H \{ \pi\chi_1^0\delta_1 [C_1\chi_1''(H) + C_2\chi_1'(H)] + \pi\chi_2^0\delta_2 [C_3\chi_2''(H) + C_4\chi_2'(H)] \}, \quad (4)$$

where $\chi''(H)$ and $\chi'(H)$ are the absorption and dispersion parts of the Lorentzians (in units of the static magnetic field) and the coefficients C are functions of the ratio σ_1/σ_2 and of d/δ_2 . We see from Eq. (4) that the EPR signal is the superposition of signals from the layer and the bulk. However, each of these components is no longer a simple Dysonian for localized spins, but a complex mixture of the χ'' and χ' as a consequence of the field reflections on the layer surface. The coefficients C have a proper asymptotic behavior [$C_{1,2}(d \rightarrow \infty) \rightarrow 1$, $C_{3,4}(d \rightarrow \infty) \rightarrow 0$, $C_{1,2}(d \rightarrow 0) \rightarrow 0$, $C_{3,4}(d \rightarrow 0) \rightarrow 1$, etc.] and may be cast in a convenient analytical form.⁷

We analyzed the EPR line shape, Eq. (4), numerically using the analytical expressions for C .⁷ The A/B ratio versus d/δ_2 for different ratios of σ_1/σ_2 , where $c_1 = 500$ ppm and $c_2 = 2000$ ppm⁸ (c_1 estimated from ΔH and I of the heated sample), is plotted in Fig. 3. The linewidths of the Lorentzians in Eq. (4) correspond to the experimental values of the limiting cases: before heat treatment and after heating for 1 h. One can see that the A/B ratio may reach very high values, of the order of 10, and is sensitive to d/δ_2 in the region $0.1 < d/\delta_2 < 2.0$ and to σ_1/σ_2 . For some values of σ_1/σ_2 , there is a region where the signal has a "reversed phase," i.e., the maximum A appears at a higher field than the minimum B (see inset in Fig. 3). The exact position of this region depends on the width of the Lorentzians in Eq. (4). By changing the width by decreasing T , we were indeed able to detect such a phase reversal.

The nonlinear change in A/B (Fig. 3) may now

be explained as a result of the change in the superposition coefficients C in Eq. (4) with the thickness of the layer. The experimental points (Fig. 3) indicate that $\sigma_1/\sigma_2 = 0.7$ is the most appropriate value for the conductivity ratio. This means that the resistivity of the near-surface layer is larger than that of the bulk.

Concerning the fit of the A/B ratio to the theoretical curves, one could not expect an exact quantitative reproduction of the experimental result in Fig. 1, since the theory is based on a simplified model: (i) We assumed a homogeneous

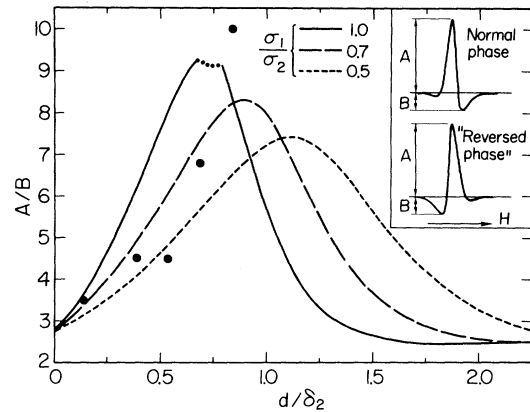


FIG. 3. Calculated A/B ratios as a function of d/δ_2 , with line shapes obtained from Eq. (4), for $c_1 = 500$ ppm and $c_2 = 2000$ ppm. The dotted part of the curve for $\sigma_1/\sigma_2 = 1.0$ represents a region of "reversed phase" (see inset for definition). The full circles represent the experimental points of the etching experiment (Fig. 1), where the thickness of the near-surface layer before etching is taken to be $0.5 \mu\text{m}$.

layer with a step-function structure, (ii) we ignored the spatial dispersion of the conductivity,⁹ and (iii) we ignored the hyperfine structure of the Er^{3+} resonance. The layer conductivity properties may also be a function of its thickness (especially, in the course of the layer formation). Nevertheless, the theory explains the origin of the unusually large values of the A/B ratio, the effect of the phase reversal of the EPR line, and gives a good approximation for the A/B dependence on the layer thickness.

Our near-surface layer model is supported by the fact that the spatial arrangement of dislocations in the interior of heavily deformed Cu single crystals has been observed to be different from that in the near-surface layer.¹⁰ The dislocations in the interior of the crystal were arranged in a well-developed cell structure, and the interiors of the cells were free of dislocations, while the dislocations in the near-surface layer were arranged in a less well-developed cell structure with long isolated dislocations threading the cells (see Fig. 6 of Ref. 10). We assumed that the above arrangement of dislocations was the one that existed in the rolled Au:Er specimen prior to annealing. Therefore, the decrease in I in the near-surface layer was interpreted as being caused by the segregation of Er ions to both the surface and the dislocations that threaded the cells [monitored in experiment (b) as a function of time]. The fact that the bulk of the EPR specimen, at a distance of $\sim 0.5 \mu\text{m}$ from the original surface, almost exhibited the initial I value implied that the diffusion coefficient of Er in Au at 400 C was not large enough for massive segregation of Er to the dislocations in the cell walls to have occurred.

In conclusion, this is the first time that the near-surface layer structure of a metallic alloy was discovered and studied by means of EPR. The technique seems to be a new and promising way of studying the metallurgical processes in some metallic alloys. The theoretical results of the

two-layer structure may also be used to explain anomalous A/B ratios obtained in EPR experiments in metals. Supplementary experimental techniques, e.g., transmission electron microscopy, might be useful in obtaining additional information on the near-surface layer.

D. N. Seidman wishes to thank the Lady Davis Foundation for a visiting professorship at the Hebrew University which helped to make this interaction possible. V. Zevin is grateful to the Max-Planck-Institut für Festkörperforschung, Stuttgart, and especially to P. Fulde for the warm hospitality. Helpful discussions with R. Orbach are gratefully acknowledged. We thank A. Grayewsky for his invaluable help in sample preparation. This work was supported in part by a grant from the U. S.-Israel Binational Science Foundation.

¹A. Raizman, J. T. Suss, D. N. Seidman, D. Shaltiel, V. Zevin, and R. Orbach, *J. Appl. Phys.* **50**, 7735 (1979).

²K. Okuda and M. Date, *J. Phys. Soc. Jpn.* **27**, 839 (1969).

³D. Davidov, C. Rettori, R. Orbach, A. Dixon, and E. P. Chock, *Phys. Rev. B* **11**, 3546 (1975).

⁴L. Landau and E. Lifschitz, *Electrodynamics of Continuous Media* (Pergamon, New York, 1960).

⁵H. Hasegawa, *Prog. Theor. Phys.* **21**, 483 (1959).

⁶J. Winter, *Magnetic Resonance in Metals* (Clarendon, Oxford, 1971).

⁷To be published.

⁸The $\sigma_1/\sigma_2 = 1$ case in Fig. 3 still shows large A/B values, because the magnetic homogeneity is absent ($\chi_1^0 \neq \chi_2^0$ and $\chi_1 \neq \chi_2$).

⁹The electron-mean free path λ which is related to the conductivity of the Au + 2000-ppm-Er specimen is about $0.07 \mu\text{m}$. For the layer and $\sigma_1/\sigma_2 = 0.7$, $\lambda \approx 0.049 \mu\text{m}$ which is smaller than both $\delta_1 \approx 0.72 \mu\text{m}$ and $d \approx 0.5 \mu\text{m}$. However, for larger σ_1/σ_2 and/or smaller d , the spatial dispersion effect may be significant.

¹⁰T. Tabata, H. Fujita, and H. Kusuhashi, *J. Phys. Soc. Jpn.* **45**, 1320 (1978).